



LAWRENCE  
LIVERMORE  
NATIONAL  
LABORATORY

# Experiences with Opto-Mechanical Systems that Affect Optical Surfaces at the Sub-Nanometer Level

L. C. Hale, J. S. Taylor

April 3, 2008

Precision Mechanical Design and Mechatronics for Sub-50 nm Semiconductor Equipment; 2008 Spring Topical Meeting for the American Society for Precision Engineering  
Berkeley, CA, United States  
April 7, 2008 through April 8, 2008

## **Disclaimer**

---

This document was prepared as an account of work sponsored by an agency of the United States government. Neither the United States government nor Lawrence Livermore National Security, LLC, nor any of their employees makes any warranty, expressed or implied, or assumes any legal liability or responsibility for the accuracy, completeness, or usefulness of any information, apparatus, product, or process disclosed, or represents that its use would not infringe privately owned rights. Reference herein to any specific commercial product, process, or service by trade name, trademark, manufacturer, or otherwise does not necessarily constitute or imply its endorsement, recommendation, or favoring by the United States government or Lawrence Livermore National Security, LLC. The views and opinions of authors expressed herein do not necessarily state or reflect those of the United States government or Lawrence Livermore National Security, LLC, and shall not be used for advertising or product endorsement purposes.

# EXPERIENCES WITH OPTO-MECHANICAL SYSTEMS THAT AFFECT OPTICAL SURFACES AT THE SUB-NANOMETER LEVEL

Layton C. Hale<sup>1</sup> and John S. Taylor<sup>2</sup>

<sup>1</sup>Innovative Machine Solutions, Brentwood, CA, USA

<sup>2</sup>Lawrence Livermore National Laboratory, Livermore, CA, USA

## INTRODUCTION

Projection optical systems built for Extreme Ultraviolet Lithography (EUVL) demonstrated the ability to produce, support and position reflective optical surfaces for achieving transmitted wavefront errors of 1 nm or less. Principal challenges included optical interferometry, optical manufacturing processes, multi-layer coating technology and opto mechanics. Our group was responsible for designing, building and aligning two different projection optical systems: a full-field, 0.1 NA, four-mirror system for 70 nm features and a small-field, 0.3 NA, two-mirror system for 30 nm features. Other than physical size and configuration, the two systems were very similar in the way they were designed, built and aligned. A key difference exists in the optic mounts, driven primarily by constraints from the metrology equipment used by different optics manufacturers. As mechanical stability and deterministic position control of optics will continue to play an essential role in future systems, we focus our discussion on opto-mechanics and primarily the optic mounts.

## BACKGROUND

A major next-generation lithography program, involving three national laboratories and members of an industrial consortium of microelectronics manufacturers, organized in 1997 to develop enabling technologies for Extreme Ultraviolet Lithography (EUVL). A main objective was realized with the construction of a prototype tool called the Engineering Test Stand (ETS), which as shown in FIGURE 1, was configured as a full-field, step-and-scan lithography tool [1, 2]. Using four mirrors with a modest 0.1 numerical aperture (NA), the system was capable of printing 70 nm features.

Within our program, a complementary project sponsored by Sematech developed a small-field, 0.3 NA, two-mirror projection optic designed to print 30 nm features. Several systems were built by us and Zeiss to be used in Micro-Exposure Tools (MET) such as that shown in FIGURE 2 [3, 4]. These development tools enabled high-resolution printing several years before high-NA, pre-

production (or beta) tools were to become available from commercial suppliers.

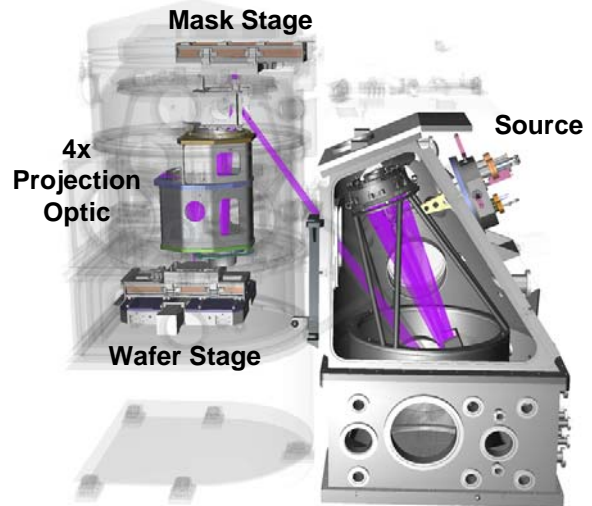


FIGURE 1. Solid model of the ETS.

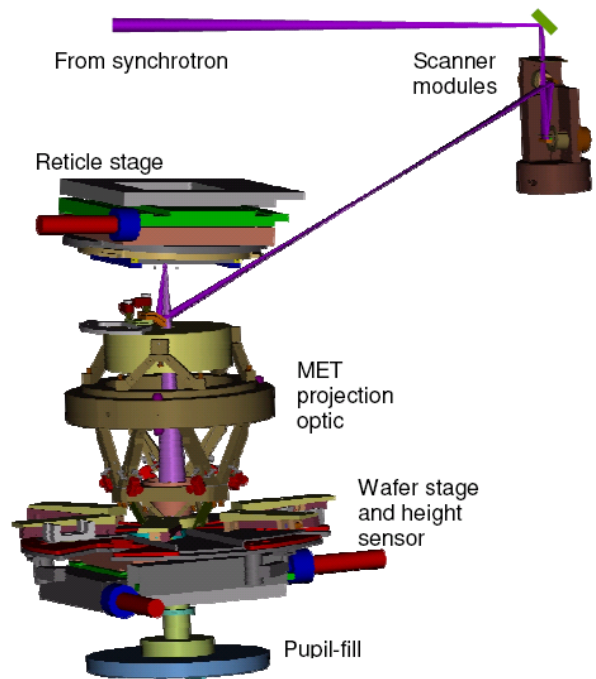


FIGURE 2. Solid model of the Microfield Exposure Station located at the Advanced Light Source, Lawrence Berkeley National Laboratory.

### Design features of the ETS projection optic

The four mirrors in the ETS projection optic are identified in the order that light reflects through the system as FIGURE 3 shows. The system has eight actuated degrees of freedom (or compensators) to facilitate fine alignment using optical interferometry as feedback. The compensators are: tip-tilt-piston actuation for both M2 and M4, and X-Y actuation for M3, where Z is vertical along the optical axis. Mechanical adjustments are provided for all the mirrors through the use of fitting spacers and clearance holes at bolted interfaces. M1, M2 and M4 are mild off-axis aspheres and are adjustable in five degrees of freedom, while the spherical M3 requires only three. All optical surfaces are axisymmetric about the optical axis, which passes through M3. The image ring field is 3 x 26 mm and concentric with the optical axis. The object ring field is 4x larger and lies on the opposite side of the optical axis. The system can be adjusted telecentric at the image plane using X-Y actuators on the aperture stop located just above M3.

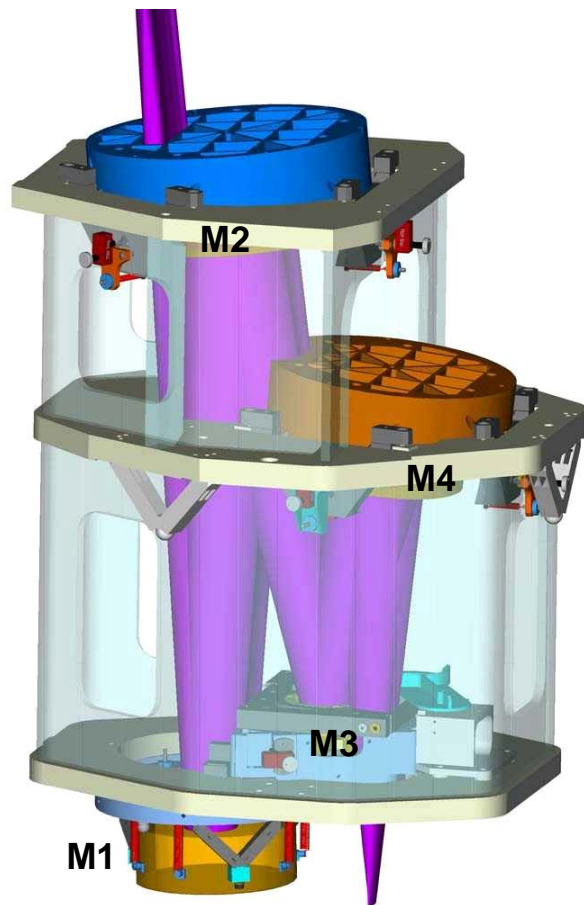


FIGURE 3. Solid model of the four-mirror ETS projection optic with 4x magnification. The size is 514 x 550 x 1075 mm (wafer to mask).

### Design features of the MET projection optic

Again identified in the order that light reflects through the system, M1 and M2 are both mild on-axis aspheres with holes cut in their centers for ray clearance. As FIGURE 4 shows, M1 is suspended from a six-degree-of-freedom hexapod, where all motions except Z rotation act as compensators for fine alignment using optical interferometry as feedback. A manual Z rotational axis allows large-angle clocking of M2 relative to M1, which may be used to cancel any astigmatism the mirrors have in common. Mechanical adjustments are provided using clearance holes and fitting spacers at the hexapod legs and clearance holes where the optic mounting flexures bolt to structures.

The image and object planes are tilted 0.8° and 4°, respectively, in order for light to enter the system off a reflective mask. The fields are rectangular, 0.2 x 0.6 mm at the wafer and 5x larger at the mask, to limit the design wavefront error to 0.42 nm RMS and the distortion to 242 nm peak. For non tilted planes over a 0.6 mm diameter image field, the design wavefront error is 0.28 nm RMS and the distortion is 2.42 nm peak.

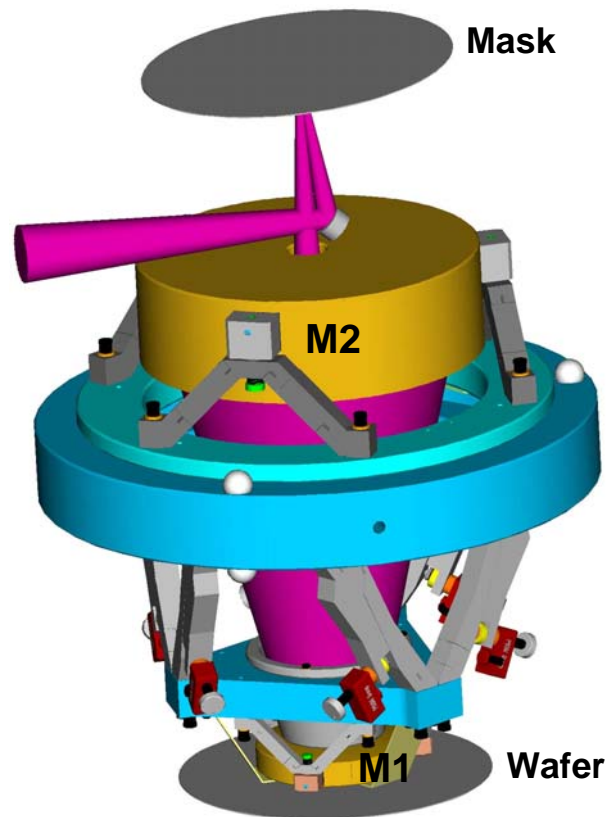


FIGURE 4. Solid model of the two-mirror MET projection optic with 5x magnification. The size is Ø360 x 474 mm (wafer to mask).

### Design features in common

Both ETS and MET projection optical systems were constructed principally from materials having low coefficients of thermal expansion (CTE) such as Zerodur for the mirrors and Super Invar for the structural components. In most cases, threaded fasteners consisted of Invar-36 threaded studs and steel nuts and washers, usually Allen nuts unless the smaller height of a hex nut was advantageous. A practical advantage of studs and nuts over cap screws is the additional freedom within the thread clearances for the nut to square itself to the surface being clamped. Particularly for the single-fastener joints prevalent in our designs, we found that tightening cap screws would at times cause the joint to move (shift and/or rotate) but not so with studs. As a rule, all these joints had shallow counterbores on either surface to relieve the bulge area around threads and to concentrate the area of contact to a larger mean radius.

Exact-constraint design principles were employed throughout these systems, including the optic mounts, the actuation stages and the interface between the projection optic and the tool. Since the total figure error allowed over the clear aperture of a mounted optic was 0.25 nm RMS and we typically allowed less than 10% of this in total to the optic mounts, this dictated a very repeatable state of stress in the optic from fabrication metrology through mounting and use. In addition, the relative positions of optics must remain very stable through final alignment and use.

The optic mounts for the ETS and MET projection optics are similar in the use of six flexural links between the mirror and a robust structure called a cell. Often referred to as bipod flexures [5], the links are arranged as three vees that connect to the mirror at three vertices and to the cell at six ends. FIGURE 5 shows a typical bipod for an ETS optic and FIGURE 6 shows a complete ETS optic mount. However the ETS and MET optic mounts differ in how the connect-disconnect functionality is implemented. The following section explains the two approaches and the rationale for each [6].

Alignment actuation was achieved on both systems using flexure stages driven by commercial piezo-screw actuators [7]. The stage configurations differed depending on the degrees of freedom required for compensation, but all incorporated mechanical advantage to increase the available force and decrease both least increment of motion and effective CTE [8, 9]. These actuators do not provide consistent step size so position feedback was provided separately using either capacitance

gauges to directly sense motion on the ETS optic cells or LVDTs embedded in the actuation flexures of the MET hexapod.

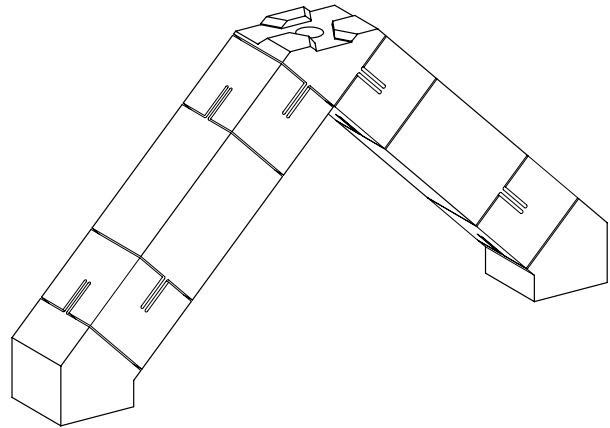


*FIGURE 5. The bipod flexure used on ETS optics has a six-constraint interface to the optic.*

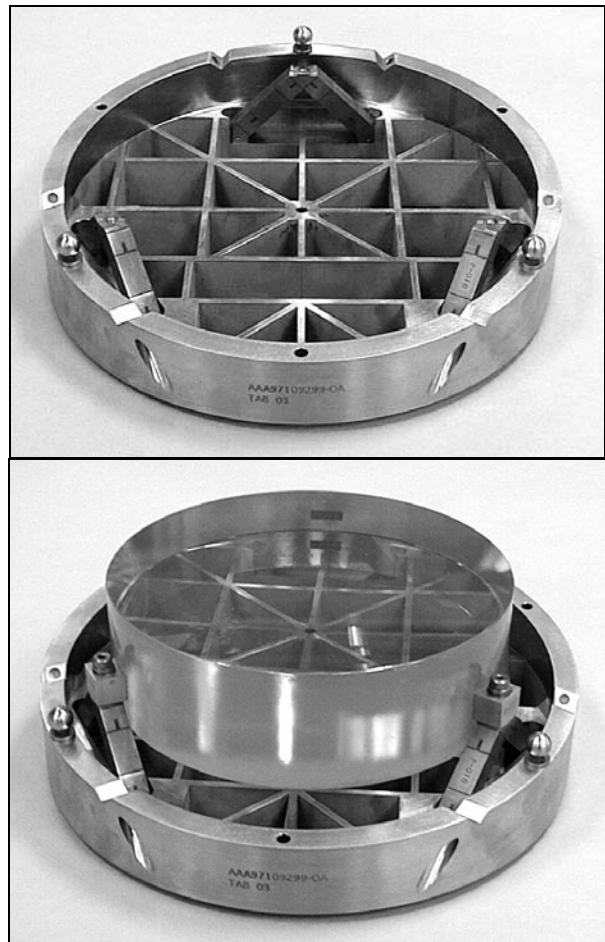


*FIGURE 6. M2 optic mount with surrogate optic installed (below). The actual M2 optic has a large cutout to clear the ray bundle.*

While both systems used a kinematic interface between the projection optic and the tool (or alignment interferometer), the substantial mass difference led to different design solutions. At 35 kg, the MET projection optic could reasonably interface using a classic three-vee kinematic coupling, with both contact stress and friction force being acceptable. Referring to FIGURE 4, three balls attach through conical seats in both the upper and lower surfaces of the ring-shaped housing. The tool would present three vees (or equivalent constraints) to the lower set of balls while the upper set is available for other equipment to stack on top.

With a mass of over 200 kg, the ETS projection optic presented three, flexure-mounted cones (equivalent to vees) that rested on three balls in the tool. This kept the contact stress low enough to use an unhardened material (Super Invar) and it reduced the friction force. A damping treatment was applied in parallel with the flexures to reduce amplification of the suspension modes of the system [10].

## **OPTIC MOUNTS**

The main functional requirements of the optic mounts are: 1) to enable reproducible fabrication metrology, 2) to preserve the optical figure achieved in manufacturing through use in the system, and 3) to hold its position stable within the system. The optical fabrication process is iterative between metrology and material removal, and for several practical reasons, we chose not to subject the optic mount to the material removal process. This choice required the optic mount to have connect-disconnect functionality. Further it would be impractical to coat the optic in the mount.

Another choice driven by schedule and the desire to keep the optics as simple as possible was to bond mounting features to the optic with epoxy. We used Super Invar blocks bonded to the outer cylinder of the optic with a nominal bond line of 0.1 mm. Concern for stability in this joint over time motivated experiments to quantify the creep rate of several candidate epoxies from which the time to drift out of alignment could be inferred [11]. We estimated 6 to 12 months and experience has shown it to be at least this long.

Designers of production tools will confront tighter surface figure and positioning tolerances, need for longer term stability and significantly higher levels of fluence. The ETS optics were measurably heated,  $> 1^\circ \text{C}$  for M1 then progressively less in sequence, but not so much as to require cooling

measures beyond radiation in the vacuum. For production-tool optic mounts, we would expect to see mounting features produced directly in the optic substrate and some means of active cooling.

## **ETS optic mounts**

The ETS optics were manufacture by Tinsley (now ASML Optics) using the PSDI Interferometer for figure metrology [12,13]. Interferometers for M2, M3 and M4 were constructed with vertical axes to test the optics in their use orientation. This allowed the more conservative strategy of using the same mounts for fabrication metrology as used in the system. As long as the mounts generate a very repeatable elastic strain within the optic, the optical fabrication process will produce the desired shape as mounted.

Gravity-induced strain is huge when the figure error budget is sub-nanometer. This requires the position and orientation of the flexure constraints to be very repeatable. A second source of strain comes from disturbance loads. Each bipod flexure has nonzero compliance in four unconstrained degrees of freedom, which can generate three moments,  $M_r$ ,  $M_t$ ,  $M_z$ , and a force,  $F_r$ , where for example, an optic is usually most sensitive to  $M_r$  (a moment about a radial axis from the optic centerline through the vertex of the bipod). Disturbance loads can arise from non repeatable coupling to the optic, differential thermal expansion and plastic deformation of the flexures, say, from accidental damage.

For the ETS optic mounts (see FIGURE 5, FIGURE 6 and FIGURE 7) a three-tooth kinematic coupling was used at each bipod to provide the requisite, highly repeatable, connect-disconnect functionality [14]. The contacting surfaces were cut into the Super Invar parts using wire EDM. Tests on this coupling showed it to be repeatable to within  $1 \mu\text{m}$  in position and  $10 \mu\text{r}$  in angle, which was well within the error budget. However over untold number of engagements, debris would accumulate in the contact area and cause non repeatability visible to the interferometer. A simple cleaning would fix the problem. We believe the debris came from wearing in of the EDM surfaces, but it also could have come from the preload spring, a design that looked simple on paper but turned out to be flawed. The spring was compressed a set distance using a shoulder screw threaded into the flexure. After repeated use, the solid lubricant (Dichronite<sup>®</sup>) would wear from the threads and cause high friction or galling. Applying too much torque to the screw caused the coupling

to disengage (as a torque-limiting slip coupling), dangerously twisting the flexure. Technicians compensated for the bad design by replacing components when the friction became high.

The flexures were manufactured with travel stops designed to guard against over deflection from simple bending but they still were vulnerable to other modes such as twisting. We required a credible means of recovering from flexure damage that might occur late in fabrication or during assembly into the system. The process of bonding the blocks to the optic was done in the optic mount with the flexures nearly in a relaxed state, that is, with minimum disturbance loads. The best way to return to this state is to repeat the bonding process. However, there is a small risk that the flexure was also damaged earlier in fabrication but went unnoticed, meaning the optic was produced correctly with a nonzero, unknown disturbance. This could be detected by observing motion of the flexures between connect and disconnect states, but we did not instigate this level of quality control.

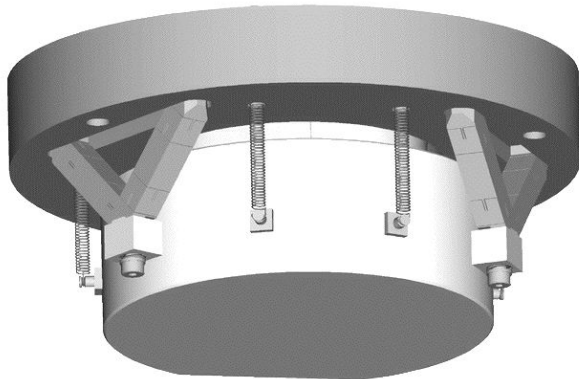


*FIGURE 7. M1 optic mount with three bipod flexure constraints and six weight-relief springs.*

M1 posed new challenges having a convex radius of curvature over 3 m. It was deemed more practical to build the M1 interferometer with a horizontal axis and to contend with the consequences by using more elaborate optic mounts. It was decided for non technical reasons to use separate mounts for fabrication metrology (with a horizontal axis) and for use in the system (with a vertical axis). A typical approach that proved satisfactory for the horizontal-axis mount is a simple band. The wrap angle was optimized using finite element analysis (FEA) to minimize non spherical deformation over the clear aperture. FIGURE 7 shows the vertical-axis mount, which supports the optic rigidly with three bipod flexures and compliantly with six additional weight-relief springs around the perimeter. This produced

primarily spherical deformation, which may be absorbed into the radius tolerance. The resulting non spherical deformation was sufficiently small with nine support points. The tension in each spring was set to one-ninth the weight of the optic using a simple apparatus with a force transducer and a positioning stage.

### **MET optic mounts**

The MET optics were produced by Zeiss using their own interferometers. The very short cavity length between the optic under test and the reference optic prevented us from using the same bipod-style mount for both fabrication metrology and use in the projection optic. Fortunately the interferometers could be set up with vertical axes to test the optics in their use orientation. Then the gravity-induced strain that is polished out of the optic in the metrology mount will be correct for the projection optic mount if both provide constraints in the same positions and orientations. This is demonstrated in FIGURE 8 and FIGURE 9. Strain from disturbance loads is best matched by driving them sufficiently toward zero for both mounts. This was analyzed in the design process using an error budget, which later became a control model for the assembly process.

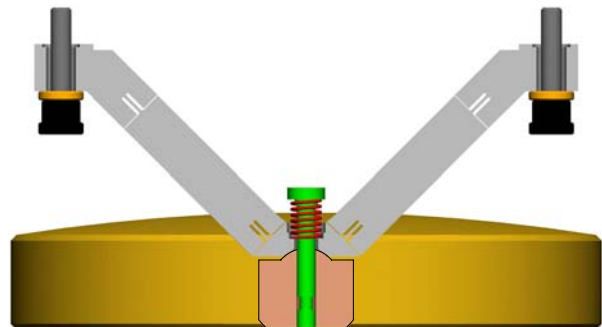


*FIGURE 8. M1 projection optic mount showing a cross section through the bipod and cone-sphere interface to the optic.*

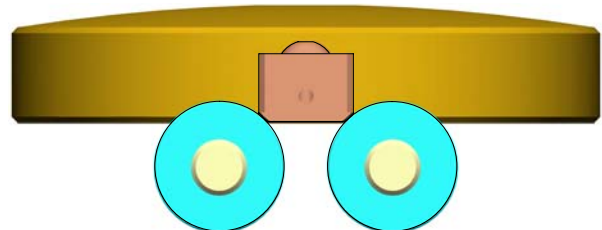


*FIGURE 9. M1 fabrication metrology mount showing equivalent constraints provided by anti-friction bearings.*

For both M1 and M2 metrology mounts, three pairs of anti-friction bearings were used to act as a low-friction, 3-V kinematic coupling. The rollers contact spherical surfaces machined into the three blocks bonded to each optic. This metrology mount performs well and is very quick and easy to use. For both M1 and M2 projection optic mounts, three bipod flexures provide constraint through the same points and in the same planes as the metrology mounts, within manufacturing tolerances. The bipods have conical sockets that interface with spheres on the bonded blocks. Referring to the figures for M1, the upper sphere that mates to the bipod is concentric with the partial spheres that contact the rollers. The downward-facing spheres for M2 serve both purposes.

Disturbance loads are minimized at assembly first by positioning the bipods so that the conical sockets match the positions of the spheres, which minimizes  $F_r$ . We used a coordinate measuring machine (CMM) for this and subsequent steps. In theory, the angular degrees of freedom at the cone-sphere interface allow  $M_r$ ,  $M_t$  and  $M_z$  to be minimized; however in practice, this can be very tedious. We used the CMM to measure the bipods before and after mounting the optic. Then we used this information to deduce the disturbance loads sprung into the flexures. Our technique to lower the optic gently onto the mount would often yield one or two disturbance loads out of bounds. At times we would resort to tapping the flexure to bring it in bounds. The joint was then preloaded with a spring to keep it in place; however, we found that friction was insufficient to prevent rotation in the joint due to normal handling. Adding a drop of epoxy would wick into the joint and prevent this rotation, yet the joint is fragile enough to separate if needed.

## ACKNOWLEDGEMENTS

This work was performed under the auspices of the U.S. Department of Energy by Lawrence Livermore National Laboratory in part under Contract W-7405-Eng-48 and in part under Contract DE-AC52-07NA27344.

## REFERENCES

- 
- [1] Tichenor, Daniel A., et al., "EUV Engineering Test Stand," SPIE Emerging Lithographic Technologies IV, 2000, **3997**  
<https://e-reports-ext.llnl.gov/pdf/237705.pdf>
- [2] Tichenor, Daniel A., et al., "System Integration and Performance of the EUV Engineering Test Stand," SPIE Emerging Lithographic

- 
- Technologies V, 2001, **4343**  
<https://e-reports-ext.llnl.gov/pdf/239913.pdf>
- [3] Naulleau, Patrick P., et al., "Extreme ultraviolet microexposures at the Advanced Light Source using the 0.3 numerical aperture micro-exposure tool optic," JVST B, 2004, **22**(6), <http://goldberg.lbl.gov/pubs/index.php>
- [4] Naulleau, Patrick P., et al., "EUV microexposures at the ALS using the 0.3-NA MET projection optics," Proc. SPIE, 2005, **5751**, <http://goldberg.lbl.gov/pubs/index.php>
- [5] Vukobratovich, Daniel and Richard, Ralph M. "Flexure mounts for high-resolution optical elements" SPIE Optomechanical and Electro-Optical Design of Industrial Systems, 1988, **959**
- [6] Hale, Layton C., "Principles and Techniques for Designing Precision Machines," Ph.D. Thesis, MIT, 2/1999 (see Chapters 6 and 7)  
<https://e-reports-ext.llnl.gov/pdf/235415.pdf>
- [7] Picomotor™ from New Focus  
<http://www.newfocus.com>
- [8] Tajbakhsh, H., et al., "Three-Degree-of-Freedom Optic Mount for Extreme Ultraviolet Lithography," Proc. ASPE, 1998, **18**  
<https://e-reports-ext.llnl.gov/pdf/235106.pdf>
- [9] Hale, Layton C., et al., "High-NA Camera for an EUVL Microstepper," Proc. ASPE, 2000, **22**, <https://e-reports-ext.llnl.gov/pdf/239974.pdf>
- [10] Jensen, J. A. and Hale, L. C., "Application of Constrained-Layer Damping to a Precision Kinematic Coupling," Proc. IMAC-19, 2001  
<https://e-reports-ext.llnl.gov/pdf/242864.pdf>
- [11] Patterson, S. R., et al., "The Dimensional Stability Of Lightly-Loaded Epoxy Joints," Proc. ASPE, 1998, **18**  
<https://e-reports-ext.llnl.gov/pdf/235105.pdf>
- [12] Sommargren, Phillion and Campbell, "Sub-nanometer interferometry for aspheric mirror fabrication," 9th International Conference on Production Engineering, 1999  
<https://e-reports-ext.llnl.gov/pdf/236193.pdf>
- [13] Sommargren, G. E., et al., "100-Picometer Interferometry for EUVL," Microlithography 2002, <https://e-reports-ext.llnl.gov/pdf/241473.pdf>
- [14] Three Tooth Kinematic Coupling, U.S. Patent 6,065,898, 5/2000